Published in final edited form as:
Arthritis Rheum. 2011 April ; 63(4): 1054–1064. doi:10.1002/art.30231.

Type I IFN-dependent CD86^{high} Marginal Zone-Precursor B Cells are Potent T-Cell Costimulators

John H. Wang, Ph.D.[1], **Qi Wu, B.S.**[1], **PingAr Yang, B.S.**[1], **Hao Li, M.S.**[1], **Jun Li, MD, Ph.D.**[1], **John D. Mountz, M.D., Ph.D.**[1,2], and **Hui-Chen Hsu, Ph.D.**[1]

[1]Department of Medicine, Division of Clinical Immunology & Rheumatology, University of Alabama at Birmingham, Birmingham, AL 35294

[2]Birmingham VA Medical Center, Birmingham, AL 35233

Abstract

Objective—To investigate the role of CD86^{high} marginal zone precursor (MZ-P) B cells in type I interferon (IFN)-induced T-dependent responses in autoimmune BXD2 mice.

Methods—Confocal imaging was used to determine the location of plasmacytoid dendritic cells (pDCs), MZ-P B cells and CD4 T cells in the spleens of BXD2 and BXD2-*Ifnar*$^{-/-}$ mice. Immunohistochemistry staining was used to determine IgG^{bright} cells in BXD2 and BXD2-*Ifnar*$^{-/-}$ spleens. ELISA was used to determine serum levels of IFN-α, autoantibody, and NP-CGG- or NP-Ficoll-induced anti-NP_2 antibody titers. Quantitative real-time (qRT)-PCR was used to determine the levels of type I IFN transcripts. [^{3}H]-thymidine was used to measure T-cell proliferation. CD86 and CD80 expression was determined by FACS.

Results—Type I IFN receptor (IFNR) deletion abrogated development of IgG^{bright} cells and suppressed a T-dependent antibody response. Type I IFN signaling is associated with the expression of CD86, but not CD80, on follicular, MZ, and MZ-P B cells. However, MZ-P B cells demonstrated the highest expression of CD86 and the highest capacity for T-cell costimulation with intact type I IFNR. This effect was blocked by an antibody that neutralizes CD86. In IFNR intact BXD2 spleens, MZ-P B cells clustered at the T-B border. CD86 deletion suppressed germinal center formation, autoantibody production, and development of autoimmune diseases in BXD2 mice.

Conclusion—Type I IFN can promote autoimmune responses in BXD2 mice through upregulation of CD86^{high} expression on MZ-P B cells and trafficking of MZ-P B cells to the T-B border to provide costimulation to CD4 T cells.

High levels of expression of type I IFN-inducible genes, known as the “type I IFN” signature, was found in the peripheral blood of SLE patients (1,2). Type I IFN is produced

Hui-Chen Hsu, PhD (Corresponding Author): Department of Medicine, Division of Clinical Immunology & Rheumatology, University of Alabama at Birmingham, 1825 University Boulevard, SHELB 311, Birmingham, AL 35294; rheu078@uab.edu.

All authors claim to have no financial interests which could create a potential conflict of interest or the appearance of a conflict of interest with regard to the work.

AUTHOR CONTRIBUTIONS

All authors were involved in drafting the article or revising it critically for important intellectual content, and all authors approved the final version to be published. Dr. Hsu had full access to all of the data in the study and takes responsibility for the integrity of the data and the accuracy of the data analysis.

Study conception and design. Wang, Mountz, and Hsu.

Acquisition of data. Wang, Wu, Yang, Li, Li, Mountz, and Hsu.

Analysis and interpretation of data. Wang, Wu, Yang, Li, Li, Mountz, and Hsu.

Final approval of the manuscript. Wang, Wu, Yang, Li, Li, Mountz, and Hsu.

primarily by $CD11c^{low}$-expressing dendritic cells (DCs) that express the phenotypic markers B220, Gr-1, and a more specific surface marker, the plasmacytoid dendritic cell antigen (PDCA-1) (3,4). These DCs are known as plasmacytoid dendritic cells (pDCs) (3–6).

T-dependent antibody response requires antigen presentation by major histocompatibility complex II and costimulation via CD80 or CD86 expressed on antigen-presenting cells (7). Studies of human peripheral blood have found increased expression levels of CD80 and CD86 on B cells from SLE patients compared to healthy individuals (8,9). The severity of lupus disease is positively correlated with the expression levels of CD80 and CD86 (9). However, only CD86 expression was significantly elevated in lupus patients with renal disease, the hallmark of SLE, while differences in CD80 levels were statistically insignificant (10). Other studies have corroborated the importance of CD86 but not CD80 by finding that only CD86 expression on B cells is elevated in patients with inactive SLE and that its level is further elevated in conjunction with active disease (11,12).

We previously demonstrated that BXD2 mice spontaneously produce pathogenic autoantibodies that can induce and exacerbate glomerulonephritis and erosive arthritis (13). Blocking of the interaction of B7-CD28 in young BXD2 mice using AdCTLA4-Ig dramatically suppressed the expression of activation-induced cytidine deaminase (AID), which is the essential enzyme to promote B-cell somatic hypermutation (SHM) and class-switch recombination (CSR) (14). This treatment also prevented the development of both nephritis and arthritis in BXD2 mice (14). Although CD86 was found to be increased in BXD2 B cells (14), it has not been specifically determined if the increased expression of CD86 is associated with the autoimmune pathogenesis in BXD2 mice. It is also unclear as to at what stage(s) of the germinal center (GC) development that $CD86^{high}$ B cells encounter $CD28^{+}$ CD4 T cells and what mechanisms are involved in driving the encounter of these cells.

Recently, we have identified a subpopulation of B cells that have the surface expression of $CD1d^{high}IgM^{high}CD21^{high}CD23^{high}$ in BXD2 mice, which are significantly increased in the spleens of BXD2 mice at the expense of reduced marginal zone (MZ) B cell counts (15). This population of $CD19^{+}$ splenocytes is commonly known as the marginal zone precursor (MZ-P) B cells (16). The immunopathogenesis for MZ-P B cells in BXD2 mice was demonstrated by their high-affinity binding for an exogenous antigen, TNP-Ficoll (15). Importantly, our previous study also showed that high levels of type I IFN produced by pDCs in the marginal sinus plays an important role in upregulating CD69 and facilitating TNP^{+} MZ-P B-cell migration to the light zone border of GCs (15).

In the current study, we examined the role of type I IFN in regulating the surface expression of costimulatory molecules, CD80 and CD86, on follicular (FO), MZ, and MZ-P B cells. We also determined if type I IFN signaling is required for MZ-P localization at the critical T-B border before a spontaneous GC response is initiated. Our present results show that type I IFN-induced upregulation of CD86 on MZ-P B cells and direction of MZ-P migration to the T-B border is important in promoting an IgG antibody response and autoimmune disease.

MATERIALS and METHODS

Mice

Female homozygous C57BL/6J (B6), BXD2 recombinant inbred, and B6-*Cd86*$^{-/-}$ mice were obtained from The Jackson Laboratory (Bar Harbor, ME); B6.*Ifnar*$^{-/-}$ mice were obtained from Dr. Jocelyn Demengeot (Instituto Gulbenkian de Ciência, Oeiras, Portugal). BXD2-*Ifnar*$^{-/-}$ and BXD2-*Cd86*$^{-/-}$ were generated by backcrossing B6-*Ifnar*$^{-/-}$ and B6-*Cd86*$^{-/-}$ with BXD2 mice for seven generations. All mice were housed in the University of

Alabama at Birmingham (UAB) Mouse Facility under specific pathogen-free conditions and all procedures were approved by the UAB Institutional Animal Care and Use Committee. Unless, specified, all mice were sacrificed at 8 to 12 weeks of age.

In vivo treatments and ELISA assays

For induction of IFN-α, 5 μg of CpG-A oligonucleotide was dissolved with 30 μL DOTAP Liposomal Transfection Reagent (F. Hoffman-La Roche, Boulder, CO) in 120 μL phosphate-buffered saline (PBS). The CpG-A:DOTAP mixture was intravenously injected into mice. IFN-α ELISA kit (PBL Biomedical, Piscataway, NJ) was used to assay serum IFN-α levels.

Immunizations were carried out by intraperitoneal injection of 50 μg chicken γ-globulin haptenated with 4-hydroxy-3-nitrophenylacetyl (NP-CGG; BioSearch Technologies) adsorbed onto 1.3 mg of alum (Sigma-Aldrich) in a total volume of 100 μL of PBS or 50 μg NP-Ficoll in PBS into mice. Antibodies to NP_2-BSA coated plates were assayed by ELISA using enzyme HRP-linked anti-mouse IgM (Southern Biotech), anti-mouse IgG_{2b} (Southern Biotech), and anti-mouse IgG_{2c} (Southern Biotech) antibodies as we previously described (17).

Urinary albumin was analyzed using a competitive Albuwell M ELISA kit (Exocell Inc) according the manufacturer's protocol (13).

Flow cytometry

For the analysis of costimulatory molecules, PE-anti-CD80 (Biolegend, San Diego, CA) or PE-anti-CD86 (Biolegend) antibodies were used. For the analysis of B-cell subpopulations, Alexa700-anti-CD19 (Biolegend), PerCP-Cy5.5-anti-CD93/AA4 (Biolegend), PE-Cy7-anti-IgM (Southern Biotechnology Associates, Birmingham, AL), FITC-anti-CD21 (Biolegend), and APC-anti-CD23 (Biolegend) antibodies were used. GC B cells were analyzed using PE-anti-Fas (Biolegend) and biotin-peanut agglutinin (PNA) (Vector Laboratories, Burlingame, CA) followed by APC-conjugated streptavidin (Biolegend). All cells are fixed in 1% paraformaldehyde/FACS solution before analysis by flow cytometry using a BD LSR II flow cytometer (BD Biosciences). The analysis was performed using FlowJo Software (Tree Star, Ashland, OR). Forward-angle light scattering was used to exclude dead and aggregated cells.

For analyses of FO, MZ, and MZ-P B cells, $CD19^+$ splenocytes were first gated. As shown in Supporting Fig. 1, for FO, MZ, and MZ-P B cells, $AA4^-IgM^{low}IgD^{high}CD21^{low}CD23^{high}$, $AA4^-IgM^{high}CD21^{high}CD23^{low}$, and $AA4^-IgM^{high}CD21^{high}CD23^{high}$ splenocytes, respectively, were gated using the method described by Allman and Pillai (18). For dose-response to IFN-α, FACS sorted FO, MZ, and MZ-P B cells were cultured with increasing doses of IFN-α (PBL Biomedical Laboratories) at 0, 200, 400, and 800 U/mL for 12 hours prior to flow cytometry analysis for $CD80^+$ or $CD86^+$ cells.

Histological and confocal imaging analysis

Frozen confocal imaging was used for the detection of CD1d, CD23, CD4, IgM, and PNA (15). For the analysis of pDC and marginal sinus location, spleen frozen sections were blocked with 10% normal rat serum and were stained with anti-PDCA1 (rat IgG_{2b}) (Miltenyi Biotec, Auburn, CA), followed by Alexa 555 dye-conjugated anti-rat IgG (Invitrogen) and Alexa488-anti-MAdCAM-1 (Biolegend). All tissue sections were mounted in Fluormount G (Southern Biotechnology Associates) and viewed with a Leica DM IRBE

inverted Nomarski/epifluorescence microscope outfitted with LeicaTCS NT (Leica Microsystems, Bannockburn, IL) laser confocal optics.

For analysis of IgM or IgG deposit in the spleens and IgG deposit in the kidneys, immunohistochemistry was performed on 10% formalin-fixed spleen tissue (4 μM) sections. Endogenous peroxidase quenching was performed by addition of 3% H_2O_2 followed by 0.25% pepsin-antigen retrieval. Tissues were subsequently blocked with 1.5% BSA, followed by incubation with HRP-linked anti-mouse IgM (Southern Biotech) and/or anti-mouse IgG (Southern Biotech) and treated with 3,3',5,5'-tetramethylbenzidine (Sigma). Tissues were imaged under an Olympus BX41 System Microscope. Quantitation of IgG^+ glomeruli was carried out using the ImageJ program (developed at the U.S. National Institutes of Health and available on the Internet at http://rsb.info.nih.gov/nih-image/). Background intensity was subtracted for each image.

Costimulatory proliferation assay

B cells from the spleens were enriched by positive selection using magnetic anti-CD19 microbeads (Miltenyi Biotech). Subsequently, $CD19^+$ B cells were sorted by flow cytometry into FO, MZ, and MZ-P B cells by the combinations of surface markers specified above via FACS sorting. For IFN-α stimulation, sorted B cells were incubated with IFN-α (400 U/mL, PBL Biomedical Laboratories) for 12 hours and washed with culture medium twice prior to irradiation. For costimulation, irradiated (3000 Rad) FO, MZ, or MZ-P B cells (5×10^5) were co-cultured with 5×10^5 MACS sorted CD4 T cells derived from the spleens of BXD2 mice at a 1:1 ratio for 48 hours in triplicate round-bottom wells in 96-well plates (Costar) in the presence of anti-CD3 (2.5 μg/mL, clone 145-2C11) plus anti-CD86 (10 μg/mL, clone GL-1), anti-CD80 (10 μg/mL, clone 16-10A1) or rat IgG2a κ isotype control (10 μg/mL, clone RTK2758). The proliferative response was measured by a standard ^{3}H-thymidine incorporation assay (17) in which 1 μCi of ^{3}H-thymidine (Perkin Elmer) was added to each well during the last 12 h of culture

RNA Quantitation

The expression of type I IFN isoforms, *Ifna1*, *Ifna4*, *Ifna11*, and *Ifnb* in peripheral blood was determined using a quantitative real-time PCR (qRT-PCR) method as we previously described (15,17). The qRT-PCR mixtures contained SYBR Green PCR Master Mix (Bio-Rad) with the following primers: *Ifna1* forward: agtgagctgacccagcagat; *Ifna1* reverse: ggtggaggtcattgcagaat; *Ifna4* forward: tctgcaatgacctccatcag; *Ifna4* reverse: tatgtcctcacagccagcag; *Ifna11* forward: cccagcagatcttgaacctc; *Ifna11* reverse: ggtggaggtcattgcagaat; *Ifnb* forward: ctccaccacagccctctc; *Ifnb* reverse: catcttctccgtcatctccatag; *Actin* forward: cgttgacatccgta; *Actin* reverse: ggaaggtggacagtgagg.

Statistical analysis

All results were shown as mean ± standard error of the mean (SEM). A two-tail *t* test was used when two groups were compared for statistical differences. ANOVA test was used when more than 2 groups were compared for statistical differences. *P* values less than 0.05 were considered significant.

RESULTS

Increased type I IFN/pDCs in lupus-prone BXD2 mice

There was increased clustering of pDCs ($PDCA1^+$, *green*) in BXD2 mice located in the MZ and outside the FO, whose boundary is demarcated by the marginal sinus, which are $MAdCAM\text{-}1^+$ (*red*) (19) compared to B6 mice (Figure 1A). Further, we observed developing GCs in BXD2 mice that were located inside the FO, with clusters of these pDCs

at the MZ (Figure 1B). Intravenous treatment with CpG-A, a known toll-like receptor 9 (TLR9) ligand, in BXD2 mice dramatically increased IFN-α serum levels in the first 2 hours, peaking at 4 hours, and dramatically declined at 12 hours (Figure 1C). Though similarly-treated B6 mice also showed a similar IFN-α level kinetics, these levels were significantly lower than those from BXD2 mice (Figure 1C).

Peripheral blood cells from untreated BXD2 and B6 mice at the different ages were assayed for different type I IFN isoform transcripts (Figure 1D). In BXD2 mice, the age groups <2 months, 9–12 months, and >1 year of age showed significantly lower *Ifna1, Ifna4,* and *Ifna11* transcript levels than do the 3–6 month age group (Figure 1D). With the exception of *Ifnb*, all type I IFN transcripts were significantly lower in B6 mice compared to BXD2 mice in matched age groups <2 months, and 3–6 months of age (Figure 1D). At older ages (> 9 months), we did not detect significant differences (Figure 1D).

Type I IFN promotes IgG class-switch

Histological analysis at 20× (Fig. 2A) and 40× (Figure 2B) magnifications of spleen tissues for the identification of IgM^{bright} and IgG^{bright} large B cells was carried out to verify that spleens of BXD2, BXD2-*Ifnar*$^{-/-}$, and B6 mice all contained IgM^{bright} large B cells (Figures 2A and B), but only BXD2 mice were able to spontaneously generate significant numbers of IgG^{bright} large B cells. In contrast, BXD2-*Ifnar*$^{-/-}$ mice had virtually undetectable IgG^{bright} cells comparable to B6 mice (Figures 2A and B). The results suggest that type I IFN mainly acts through a GC-dependent mechanism to promote autoimmunity in BXD2 mice.

Type I IFN promotes a T-dependent antibody response

To differentiate if type I IFN mainly promotes a T-dependent or a T-independent antibody response, B6, BXD2, and BXD2-*Ifnar*$^{-/-}$ mice were immunized with either a known T-dependent or T-independent antigen, NP-CGG or NP-Ficoll, respectively, and intravenously treated with either placebo or CpG-A 17 hours later (Figure 3). T-dependent NP-CGG induced dramatically higher levels of high affinity IgG_{2b} and IgG_{2c} anti-NP_2 antibody isotypes in BXD2 mice compared to normal B6 mice (Figures 3B and C), while IgM titers remained low (Fig. 3A). CpG-A treatment further significantly increased high affinity IgG isotype anti-NP_2 titers for BXD2 mice compared with non-treated NP-CGG immunized controls (Figures 3B and C). Deletion of type I IFNR in BXD2 mice suppressed IgG_{2b} and IgG_{2c} titers (Figures 3B and C), regardless of treatment with CpG-A or not, indicating that intact type I IFNR is required to complete a T-dependent antibody response. NP-Ficoll did not dramatically increase IgG titers (Figures 3B and C) but generate substantial IgM titers (Figure 3A). In the presence of an intact IFNR, or CpG-A stimulation, type I IFN signaling did not significantly class-switch IgM to IgG in response to NP-Ficoll challenge (Figure 3A). These results suggest that type I IFN promotes a T-dependent antibody response and that type I IFN may play a significant role at the pre-GC stage, prior to antibody maturation and plasma cell differentiation.

MZ-P-induced T-cell costimulation and positioning is type I IFN-associated

We previously showed that the FO-oriented migration response of MZ-P B cells into the light zone border of well-formed GCs is highly associated with type I IFN (15). We now investigate the location of MZ-P B cells at the pre-GC stage. Histological analysis of spleen sections from BXD2 mice demonstrate that MZ-P B cells form clusters adjacent to CD4 T cells at the T-B boundary (Figure 4A, *top*). The boxed area in Fig. 4A is magnified to demonstrate the close proximity of the MZ-P cluster adjacent to CD4 T cells (Figure 4A, *top right*). The significant presence of clustering MZ-P B cells adjacent to CD4 T cells in BXD2 mice is in dramatic contrast to the poor MZ-P clustering observed in BXD2-*Ifnar*$^{-/-}$ at the

T-B boundary (Figure 4A, *bottom*). Instead, in BXD2-*Ifnar*$^{-/-}$ mice, the pool of B cells clustered at the T-B border is biased towards a predominant FO B cells (Figure 4A, *bottom*).

To test the CD4 T cell costimulatory capability of each of the B-cell subpopulations, we sorted and co-cultured irradiated B-cell subpopulations from BXD2 or BXD2-*Ifnar*$^{-/-}$ mice with anti-CD3 stimulated CD4 T cells. Consistent with the literature (20), MZ B cells make better costimulatory agents than do FO B cells (Figure 4B). MZ-P B cells from BXD2 mice, however, provided the greatest costimulation of CD4 T cells, compared to costimulation provided by MZ or FO B cells (Figure 4B). MZ-P B cells from BXD2-*Ifnar*$^{-/-}$ mice demonstrated significantly attenuated T-cell costimulation compared to BXD2 MZ-P B cells (Figure 4B). MZ B cells also displayed attenuated costimulatory capability when type I IFNR was deleted (Figure 4B).

Consistent with these results, there was a significantly increased percentage of CD86^{high} MZ-P compared to MZ, and FO B cells in BXD2 mice (Figure 4C). BXD2-*Ifnar*$^{-/-}$ mice exhibited an approximate 50% decrease in CD86^{high} expression by all B-cell subpopulations (Figure 4C). Interestingly, BXD2-*Ifnar*$^{-/-}$ MZ-P B cells maintained a higher basal CD86 surface expression than did their MZ and FO B cell counterparts (Figure 4C). Both MZ and MZ-P B cells maintained higher CD80 expression than did FO B cells (Figure 4D). However, CD80 expression in all 3 subpopulations of B cells was not significantly different between BXD2 and BXD2-*Ifnar*$^{-/-}$ mice (Figure 4D).

Type I IFN stimulates the costimulatory function of MZ-P via the induction of CD86

To test whether IFN-α has a direct effect on CD86 surface expression, splenic MZ-P, MZ, and FO B cells from BXD2 and BXD2-*Ifnar*$^{-/-}$ were sorted and left unstimulated or stimulated IFN-α. CD86 surface expression on all three B-cell subpopulations was determined 12 hr after stimulation with IFN-α (Figure 5A). MZ-P B cells exhibited the highest expression of CD86 compared with either FO or MZ B cells in response to IFN-α. Type I IFNR deletion showed significant blunting of CD86 expression, especially on MZ-P B cells (Figure 5A). In contrast, CD80 surface expression on FO, MZ, or MZ-P B cells was not dependent on IFN-α signaling (Figure 5A).

Stimulation of FO, MZ, and MZ-P B cells by increasing doses of IFN-α (0, 200, 400, 800 U/mL) demonstrated a dose-related upregulation of CD86 surface expression (Figure 5B, *left*) for FO, MZ, and MZ-P B cells, but most significantly on MZ-P B cells, whereas no upregulation was observed for CD80 surface expression (Figure 5B, *right*) on all three B cell subpopulations.

To test whether type I IFN promotes CD4 T cell costimulatory capability of each of the B cell subpopulations via increased expression of CD86, sorted B cells were stimulated with IFN-α and then co-cultured with anti-CD3 stimulated CD4 T cells, in the presence of rat IgG2a κ isotype control, anti-CD86, or anti-CD80. IFN-α pre-stimulated MZ-P B cells exhibited the most dramatic effect in promoting anti-CD3-induced T-cell proliferative response (Figure 5C), with lesser T-cell proliferative response by IFN-α stimulation of either MZ or FO B cells (Figure 5C). Anti-CD86 antibody effectively blocked T-cell costimulation by MZ-P B cells that were either with or without IFN-α pre-stimulation (Figure 5C). In contrast, anti-CD80 did not significantly block T-cell costimulation provided by MZ-P B cells (Figure 5C).

CD86 is essential for BXD2 autoimmune disease

To demonstrate that CD86 is a key pathogenic molecule in the induction of autoimmune disease, the phenotype of BXD2-*Cd86*$^{-/-}$ mice was determined. CD86 deletion significantly reduced spleen weight and cell count (Figure 6A). IgG autoantibodies to histone, BiP, and

DNA, were significantly reduced in BXD2-*Cd86*$^{-/-}$ mice, compared with that in BXD2 mice (Figure 6B). Histological analysis confirms that in BXD2-*Cd86*$^{-/-}$ mice, there was a dramatically reduced generation of IgG^{bright} cells in the spleen (Figure 6C). Flow cytometry and histological analyses showed significantly reduced PNA^{+} GC B cells in BXD2-*Cd86*$^{-/-}$, compared with BXD2 mice (Figure 6D). Consistent with these findings, there were dramatically diminished mesangial proliferation, diminished IgG containing immune complexes deposited in the glomeruli of the kidney (Supporting Figure 2A) and significantly diminished urinary albumin (Supporting Figure 2B) from BXD2-*Cd86*$^{-/-}$ mice at 10-mo-old, compared with age-matched BXD2 mice. BXD2-*Cd86*$^{-/-}$ mice also developed dramatically decreased erosive arthritis, characterized by significantly lower levels of inflammatory infiltration, synovial hyperplasia, and marginal erosion, compared to arthritis developed by wild-type BXD2 mice (Supporting Figure 2C and D).

DISCUSSION

Type I IFN is known to be required for autoantibody production (21). Deletion of the type I IFNR eliminated the development of autoantibodies in various murine models of lupus (22–24). Though studies conducted in non-autoimmune hosts have been proposed as pathways by which type I IFNs drive antibody responses in lupus (21), the precise mechanism by which type I IFNs generate autoantibodies is not clear. The dominant paradigm is that type I IFNs generate autoantibodies in lupus by directly promoting the maturation of autoreactive B cells into antibody-secreting plasmablasts (4,25). While this paradigm may hold true, our studies suggest additional or alternative mechanisms by which type I IFNs generate plasmablasts and/or plasma cells by promoting T-dependent autoantibody responses.

We have found increased pDCs located in clustering layers of cells in the MZ outside the FO, which is demarcated by MAdCAM-1. Consistent with a non-inflammatory phenotype, pDCs in B6 mice exhibited significantly less clustering in the MZ, and a more diffuse distribution inside the FO. However, in BXD2 mice, clustering pDCs were found in the MZ, consistent with an inflammatory environment in which immune complexes carrying TLR-binding deoxynucleoproteins may trigger pDC-induced type I IFNs and pDC clustering in the MZ (26). Because pDCs are also systemically circulated between the peripheral blood and the secondary lymphoid organs (27), significant amounts of type IFN transcripts were also found in the peripheral blood in BXD2 mice. CpG-A induction further confirms that BXD2 mice have the potential to generate high serum levels of IFN-α. Previously, we have demonstrated that the spleens of BXD2 mice have increased counts of type I IFN producing pDCs compared to normal B6 mice (15). The mRNA levels of most *Ifna* species increase until 6 months, at which age, the levels peak, and subsequently decline. Interestingly, these mRNA levels increase and peak in the same age range as do certain autoantibodies (13), consistent with our findings that type I IFNs can modulate CD4 T-cell costimulation and induce antibody responses. Declining type I IFN message levels in older BXD2 mice (>9 months) may be due to senescing/maturing pDCs in response to antigen exposure (28) and in response to an increasing antigen-autoantibody load in aging BXD2 mice (13).

We observed that intact type I IFN signaling is required for formation of IgG^{bright} large size plasmablast or plasma B cell formation. Deletion of type I IFNR in the BXD2 background eliminated the presence of IgG^{bright} B cells, while keeping the presence of IgM^{bright} B cells intact, a finding that would not be expected if type I IFNs were only responsible for maturing antibody-producing B cells into plasmablasts. Immunization with a T-dependent antigen but not a T-independent antigen shows that type I IFN can produce a high affinity IgG antibody response. Also, the T-dependent response was significantly dependent upon CpG-A induction of IFN-α. Deletion of type I IFNR, in spite of CpG-A treatment, suppressed IgG titers to baseline levels. Our findings suggest that type I IFN can promote

the generation of plasmablasts or plasma B cells in addition to their effects to induce post-GC B cell maturation.

Previous results showed that costimulation of CD4 T cells that is blocked, for instance by CTLA4-Ig, which competitively binds to either CD80 or CD86, anergizes CD4 T cells (29). The finding that B cells from SLE human subjects display high levels of costimulatory receptors, especially CD86, corroborates the assertion that the T-dependent humoral response plays a prominent role in generating autoantibodies (8–12). BXD2 mice display an autoantibody response that is significantly dependent upon costimulation signaling brought about by CD80/86-CD28 interactions as AdCTLA4-Ig treatment in BXD2 mice almost completely blocked the expression of the gene encoding AID and autoantibody production (14). As demonstrated in the current study, CD86 expression is especially important in the autoimmune phenotype of BXD2 mice. Deletion of CD86 significantly inhibited GC formation, suppressed the presence of IgG^{bright} class switched cells, attenuated autoantibody titers, and obviated the natural course of glomerulonephritis and erosive arthritis in BXD2 mice.

In the secondary lymphoid organs, such as the spleen, consist of a heterogeneous assortment of B cells (30–32). Most of these consist of mature FO B cells and a smaller population of MZ B cells, with a series of “transitional” B cells or “intermediates”, including the MZ-P B cells (32). We have previously shown that this FO-oriented migration of MZ-P B cells can be regulated via the type I IFN-induced CD69-dependent $S1P_1$ down-regulation and that MZ-P B cells can transport antigens to the light zone end of existing GCs (15). In the present study, we further demonstrated that MZ-P B cells exhibit close physical contact with CD4 T cells at the T-B border during the pre-GC stage. The deletion of type I IFNR redistributes MZ-P B cells away from this T-B border and towards the MZ. This result, together with our previous finding (15), suggest that type I IFN plays an important role to promote the FO-oriented migration of MZ-P B cells both before and after the onset of the spontaneous GC response is initiated in BXD2 mice.

The present study further shows that an important function of type I IFN-promoted MZ-P B cells at the T-B border is for the provision of costimulation to CD4 T cells. MZ B cells have been reported to express higher levels of CD86 and higher costimulation of CD4 T cells compared to FO B cells (20). We observed that MZ-P B cells have higher CD86 expression compared to either FO or MZ, and MZ-P B cells provide even stronger costimulation to CD4 T cells than MZ B cells. Significantly, CD86 expression on B cells is under the regulation of type I IFN, while CD80 is not. Disruption of type I IFN signaling lowered CD86 expression on FO, MZ, and MZ-P B cells. Although MZ-P B cells retained higher levels of CD86 in spite of disrupted type I IFN signaling compared with MZ or FO B cells, diminished CD86 expression with type I IFNR deletion significantly decreased MZ-P-induced T-cell costimulation to levels comparable to those induced by FO or MZ B cells. These results suggest that there is a critical CD86 expression threshold below which T cell costimulation becomes ineffective, and that the signal provided by type I IFN is important to elevate the expression of CD86 to levels above this threshold. Anti-CD28 costimulation normalized the costimulatory effects of MZ-P B cells, with or without IFN-α pre-stimulation, on CD4 T cell proliferation (data not shown), suggesting IFN-α mainly act through the CD86 pathway to enhance the costimulatory function of MZ-P B cells. Interestingly, CD80 expression is not under the regulation of type I IFN, and appears to not offer as strong a costimulatory molecule compared with CD86, at least in BXD2 mice. Our observation that these highly potent $CD86^{high}$ MZ-P costimulators cluster at the splenic T-B border in BXD2 mice provides the geographical advantage of providing costimulation in the very initial stages of GC formation.

In summary, our study proposes that type I IFN can offer a new avenue by which T-dependent antibody responses are generated. First, type I IFN is critical in bringing MZ-P B cells to the T-B border into the FO interior at the pre-GC stage. Second, type I IFN significantly increases the levels of CD86 on MZ-P B cells, providing potent costimulation to activated CD4 T cells. This dual-level function of type I IFN prior to the formation of GCs offers new insights into how type I IFNs can induce T-dependent autoreactive antibody responses in lupus-prone BXD2 mice and ultimately, perhaps, in human SLE.

Supplementary Material

Refer to Web version on PubMed Central for supplementary material.

Acknowledgments

We thank Dr. Jocelyn Demengeot at the Instituto Gulbenkian de Ciência in Oeiras, Portugal to provide B6-*Ifnar*$^{-/-}$ mice. We thank Ms. Enid Keyser of the Analytic and Preparative Cytometry Facility - UAB Rheumatic Diseases Core Facility (P30 AR48311) and Mr. Marion L. Spell of the UAB Center for AIDS FACS Core (P30 AI027767) for operating the FACS instrument. Confocal imaging was carried out at the Arthritis and Musculoskeletal Disease Center High Resolution Imaging Facility (P30 AR48311). P30 AI027767-23, P30 AI027767-24, and P30 AI27767-22S1 (PI: Michael Saag)

This work was supported by the American College of Rheumatology Research and Education Foundation for the *Within Our Reach: Finding a Cure for Rheumatoid Arthritis* campaign, the Alliance for Lupus Research – Target Identification in Lupus program, the Department of Veterans Affairs Merit Review Grant 1I01BX000600-01, Daiichi-Sankyo Co., Ltd, the National Institutes of Health Grants 1AI 071110-01A1 and ARRA 3RO1AI71110-02S1 (all to J.D.M.), the Lupus Research Institute Novel Research project and the Arthritis Investigator Award supported by the Arthritis Foundation (to H.-C.H).

REFERENCES

1. Bengtsson AA, Sturfelt G, Truedsson L, Blomberg J, Alm G, Vallin H, et al. Activation of type I interferon system in systemic lupus erythematosus correlates with disease activity but not with antiretroviral antibodies. Lupus. 2000; 9(9):664–671. [PubMed: 11199920]
2. Bennett L, Palucka AK, Arce E, Cantrell V, Borvak J, Banchereau J, et al. Interferon and granulopoiesis signatures in systemic lupus erythematosus blood. J Exp Med. 2003; 197(6):711–723. [PubMed: 12642603]
3. Nakano H, Yanagita M, Gunn MD. CD11c(+)B220(+)Gr-1(+) cells in mouse lymph nodes and spleen display characteristics of plasmacytoid dendritic cells. J Exp Med. 2001; 194(8):1171–1178. [PubMed: 11602645]
4. Colonna M, Trinchieri G, Liu YJ. Plasmacytoid dendritic cells in immunity. Nat Immunol. 2004; 5(12):1219–1226. [PubMed: 15549123]
5. Asselin-Paturel C, Brizard G, Pin JJ, Briere F, Trinchieri G. Mouse strain differences in plasmacytoid dendritic cell frequency and function revealed by a novel monoclonal antibody. J Immunol. 2003; 171(12):6466–6477. [PubMed: 14662846]
6. Siegal FP, Kadowaki N, Shodell M, Fitzgerald-Bocarsly PA, Shah K, Ho S, et al. The nature of the principal type 1 interferon-producing cells in human blood. Science. 1999; 284(5421):1835–1837. [PubMed: 10364556]
7. Wang S, Chen L. T lymphocyte co-signaling pathways of the B7-CD28 family. Cell Mol Immunol. 2004; 1(1):37–42. [PubMed: 16212919]
8. Wong CK, Lit LC, Tam LS, Li EK, Lam CW. Aberrant production of soluble costimulatory molecules CTLA-4, CD28, CD80 and CD86 in patients with systemic lupus erythematosus. Rheumatology (Oxford). 2005; 44(8):989–994. [PubMed: 15870153]
9. Dolff S, Wilde B, Patschan S, Durig J, Specker C, Philipp T, et al. Peripheral circulating activated b-cell populations are associated with nephritis and disease activity in patients with systemic lupus erythematosus. Scand J Immunol. 2007; 66(5):584–590. [PubMed: 17868260]

10. Liu W, Li J. Expression of CD80/CD86 and CTLA-4 mRNA in peripheral blood mononuclear cells of the patients with systemic lupus erythematosus. J Huazhong Univ Sci Technolog Med Sci. 2004; 24(3):247–249. [PubMed: 15315339]
11. Bijl M, Horst G, Limburg PC, Kallenberg CG. Expression of costimulatory molecules on peripheral blood lymphocytes of patients with systemic lupus erythematosus. Ann Rheum Dis. 2001; 60(5):523–526. [PubMed: 11302879]
12. Folzenlogen D, Hofer MF, Leung DY, Freed JH, Newell MK. Analysis of CD80 and CD86 expression on peripheral blood B lymphocytes reveals increased expression of CD86 in lupus patients. Clin Immunol Immunopathol. 1997; 83(3):199–204. [PubMed: 9175908]
13. Hsu HC, Zhou T, Kim H, Barnes S, Yang P, Wu Q, et al. Production of a novel class of polyreactive pathogenic autoantibodies in BXD2 mice causes glomerulonephritis and arthritis. Arthritis Rheum. 2006; 54(1):343–355. [PubMed: 16385526]
14. Hsu HC, Wu Y, Yang P, Wu Q, Job G, Chen J, et al. Overexpression of activation-induced cytidine deaminase in B cells is associated with production of highly pathogenic autoantibodies. J Immunol. 2007; 178(8):5357–5365. [PubMed: 17404321]
15. Wang JH, Li J, Wu Q, Yang P, Pawar RD, Xie S, et al. Marginal zone precursor B cells as cellular agents for type I IFN-promoted antigen transport in autoimmunity. J Immunol. 2010; 184(1):442–451. [PubMed: 19949066]
16. Srivastava B, Quinn WJ 3rd, Hazard K, Erikson J, Allman D. Characterization of marginal zone B cell precursors. J Exp Med. 2005; 202(9):1225–1234. [PubMed: 16260487]
17. Hsu HC, Yang P, Wang J, Wu Q, Myers R, Chen J, et al. Interleukin 17-producing T helper cells and interleukin 17 orchestrate autoreactive germinal center development in autoimmune BXD2 mice. Nat Immunol. 2008; 9(2):166–175. [PubMed: 18157131]
18. Allman D, Pillai S. Peripheral B cell subsets. Curr Opin Immunol. 2008; 20(2):149–157. [PubMed: 18434123]
19. Kraal G, Schornagel K, Streeter PR, Holzmann B, Butcher EC. Expression of the mucosal vascular addressin, MAdCAM-1, on sinus-lining cells in the spleen. Am J Pathol. 1995; 147(3):763–771. [PubMed: 7677187]
20. Attanavanich K, Kearney JF. Marginal zone, but not follicular B cells, are potent activators of naive CD4 T cells. J Immunol. 2004; 172(2):803–811. [PubMed: 14707050]
21. Ronnblom L, Alm GV, Eloranta ML. Type I interferon and lupus. Curr Opin Rheumatol. 2009; 21(5):471–477. [PubMed: 19525849]
22. Agrawal H, Jacob N, Carreras E, Bajana S, Putterman C, Turner S, et al. Deficiency of type I IFN receptor in lupus-prone New Zealand mixed 2328 mice decreases dendritic cell numbers and activation and protects from disease. J Immunol. 2009; 183(9):6021–6029. [PubMed: 19812195]
23. Nacionales DC, Kelly-Scumpia KM, Lee PY, Weinstein JS, Lyons R, Sobel E, et al. Deficiency of the type I interferon receptor protects mice from experimental lupus. Arthritis Rheum. 2007; 56(11):3770–3783. [PubMed: 17968932]
24. Santiago-Raber ML, Baccala R, Haraldsson KM, Choubey D, Stewart TA, Kono DH, et al. Type-I interferon receptor deficiency reduces lupus-like disease in NZB mice. J Exp Med. 2003; 197(6): 777–788. [PubMed: 12642605]
25. Jego G, Palucka AK, Blanck JP, Chalouni C, Pascual V, Banchereau J. Plasmacytoid dendritic cells induce plasma cell differentiation through type I interferon and interleukin 6. Immunity. 2003; 19(2):225–234. [PubMed: 12932356]
26. Asselin-Paturel C, Brizard G, Chemin K, Boonstra A, O'Garra A, Vicari A, et al. Type I interferon dependence of plasmacytoid dendritic cell activation and migration. J Exp Med. 2005; 201(7): 1157–1167. [PubMed: 15795237]
27. Yoneyama H, Matsuno K, Zhang Y, Nishiwaki T, Kitabatake M, Ueha S, et al. Evidence for recruitment of plasmacytoid dendritic cell precursors to inflamed lymph nodes through high endothelial venules. International Immunology. 2004; 16(7):915–928. [PubMed: 15159375]
28. McKenna K, Beignon AS, Bhardwaj N. Plasmacytoid dendritic cells: linking innate and adaptive immunity. J Virol. 2005; 79(1):17–27. [PubMed: 15596797]

29. Mirshahidi S, Huang C-T, Sadegh-Nasseri S. Anergy in Peripheral Memory Cd4+ T Cells Induced by Low Avidity Engagement of T Cell Receptor. The Journal of Experimental Medicine. 2001; 194(6):719–732. [PubMed: 11560989]

30. Lopes-Carvalho T, Kearney JF. Development and selection of marginal zone B cells. Immunol Rev. 2004; 197:192–205. [PubMed: 14962196]

31. Martin F, Kearney JF. Positive selection from newly formed to marginal zone B cells depends on the rate of clonal production, CD19, and btk. Immunity. 2000; 12(1):39–49. [PubMed: 10661404]

32. Pillai S, Cariappa A. The follicular versus marginal zone B lymphocyte cell fate decision. Nat Rev Immunol. 2002; 9(11):767–777. [PubMed: 19855403]

ABBREVIATIONS

AID	activation-induced cytidine deaminase
CSR	class-switch recombination
FO	follicular
GC	germinal center
IC	immune complexes
MAdCAM-1	mucosal addressin cell adhesion molecule-1
MZ	marginal zone
MZ-P	marginal zone precursor
NP-CGG	4-hydroxy-3-nitrophenylacetyl chicken gamma globulin
pDCs	plasmacytoid dendritic cells
PNA	peanut agglutinin
RA	rheumatoid arthritis
SHM	somatic hypermutation
SLE	systemic lupus erythematosus

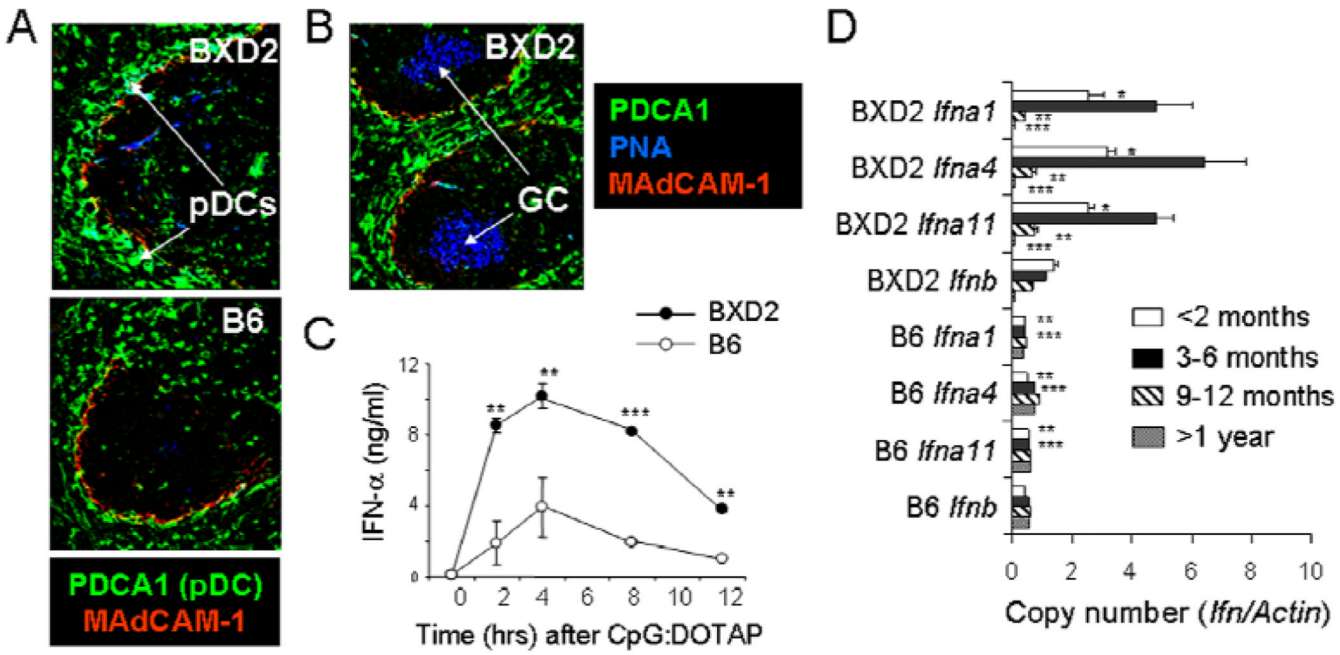

Figure 1.

Activated pDCs and type I IFN in BXD2 mice. **A**, Images of spleen sections taken from a representative BXD2 mouse and a B6 mouse stained with anti-PDCA1 (pDC, green), MAdCAM-1 (red). **B**, Representative spleen section from a BXD2 mouse with PNA^+ GC (blue) inside follicles demarcated with MAdCAM-1 (red) and surrounded by layers of pDCs (green). **C**, CpG-A:DOTAP was i.v. injected into BXD2 and B6 mice as described in Materials and Methods. Serum IFN-α levels assayed by ELISA collected at the indicated times (N=3–6, **p<0.01, ***p<0.001 between B6 and BXD2 at the same time point). **D**, RNA was extracted from peripheral blood cells. Transcripts of *Ifna1*, *Ifna4*, *Ifna11*, and *Ifnb* isoforms from BXD2 and B6 mice at different age groups were quantitated relative to copy counts of *Actin*, as described in Materials and Methods (N=6, *p<0.05, **p<0.01, ***p<0.001 noted with BXD2 age groups were compared to BXD2 at the 3–6 months of age, or in the case of B6, **p<0.01, and ***p<0.001 compared to age group-matched BXD2 mice).

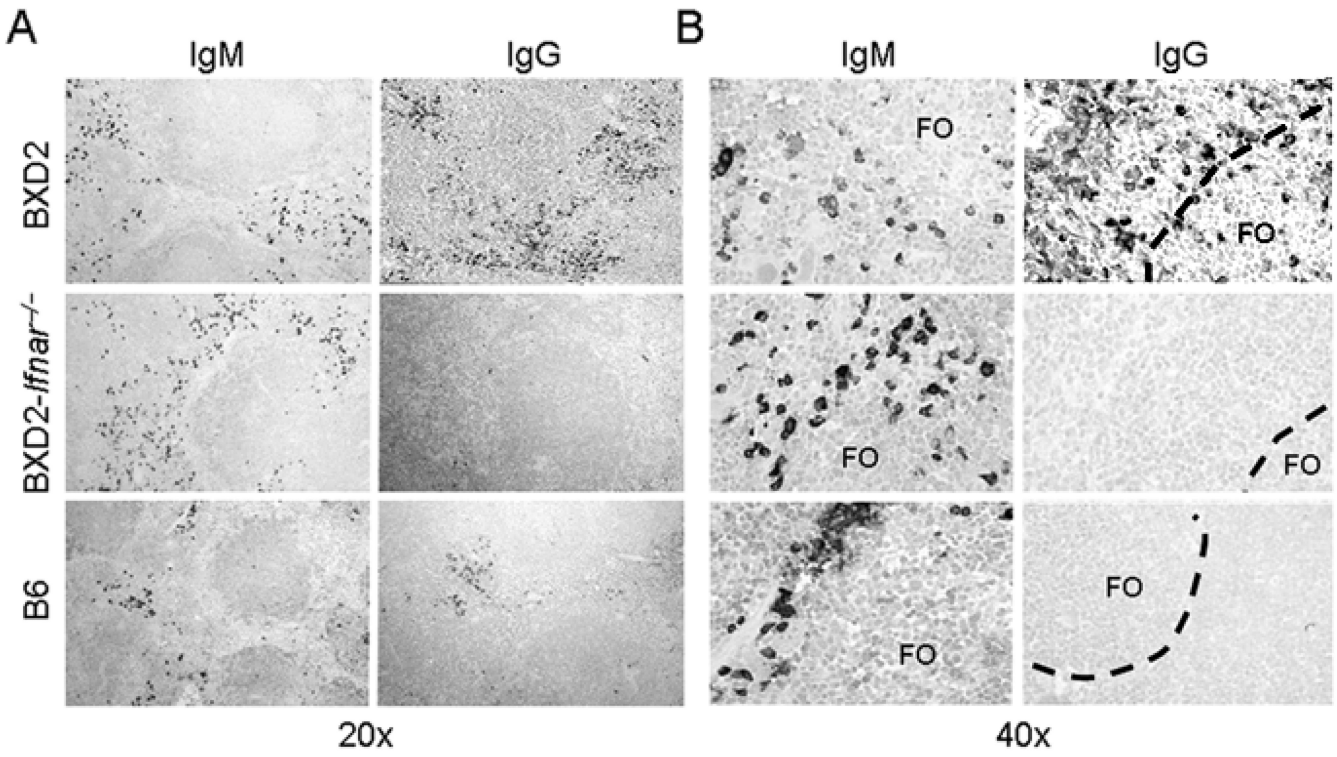

Figure 2.

Type I IFNR deletion abrogates IgG class-switch in 4-mo-old BXD2 mice. Representative spleen sections of BXD2, BXD2-*Ifnar*$^{-/-}$, and B6 mice were stained with anti-IgM and anti-IgG antibodies as described in Materials and Methods. **A**, 20× objective lens magnification of images of spleen sections showing the presence of follicles and IgM^{bright} or IgG^{bright} B cells. **B**, 40× objective lens magnification of images of spleen sections, denoted with respect to the presence of a follicle (FO) whose boundary is denoted by broken lines.

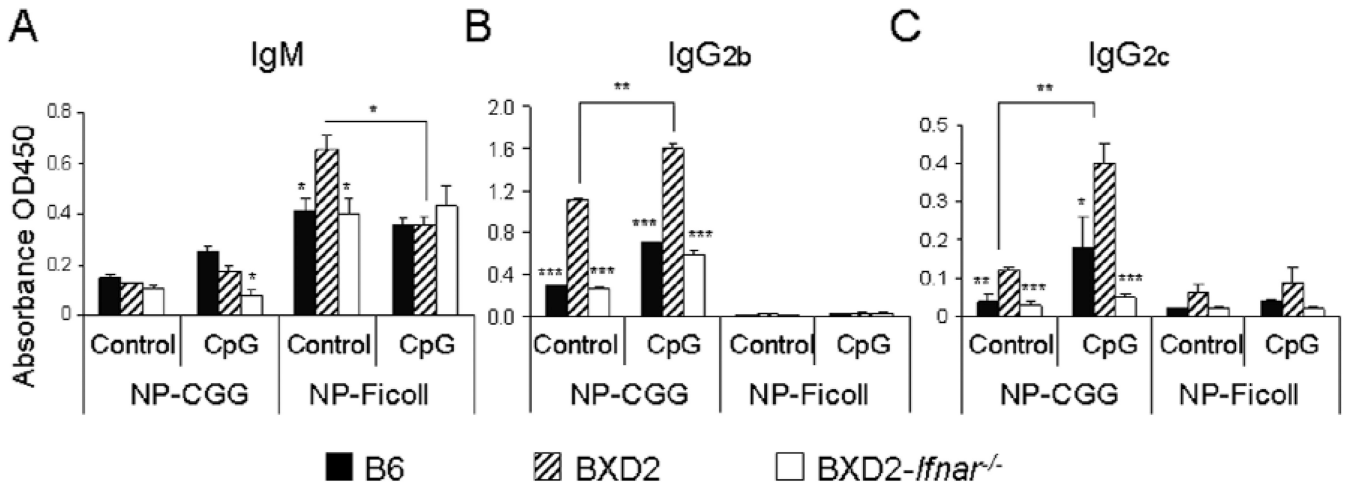

Figure 3.

Type I IFNR deletion abrogates the T-dependent antibody response. B6, BXD2, and BXD2-*Ifnar*$^{-/-}$ mice were immunized with either NP-CGG or NP-Ficoll. Seventeen hours later, the mice were either treated with placebo or CpG-A as described in Materials and Methods. Sera were collected on day 17 after immunization. IgM (A), IgG2b (B), IgG2c (C) titers of anti-NP_2, as measured by O.D. units, were assayed by ELISA (N=6, *p<0.05, **p<0.01 for CpG-A treated vs untreated BXD2 mice, *p<0.05, **p<0.01, ***p<0.001 for B6 or BXD2-*Ifnar*$^{-/-}$ vs. BXD2 mice).

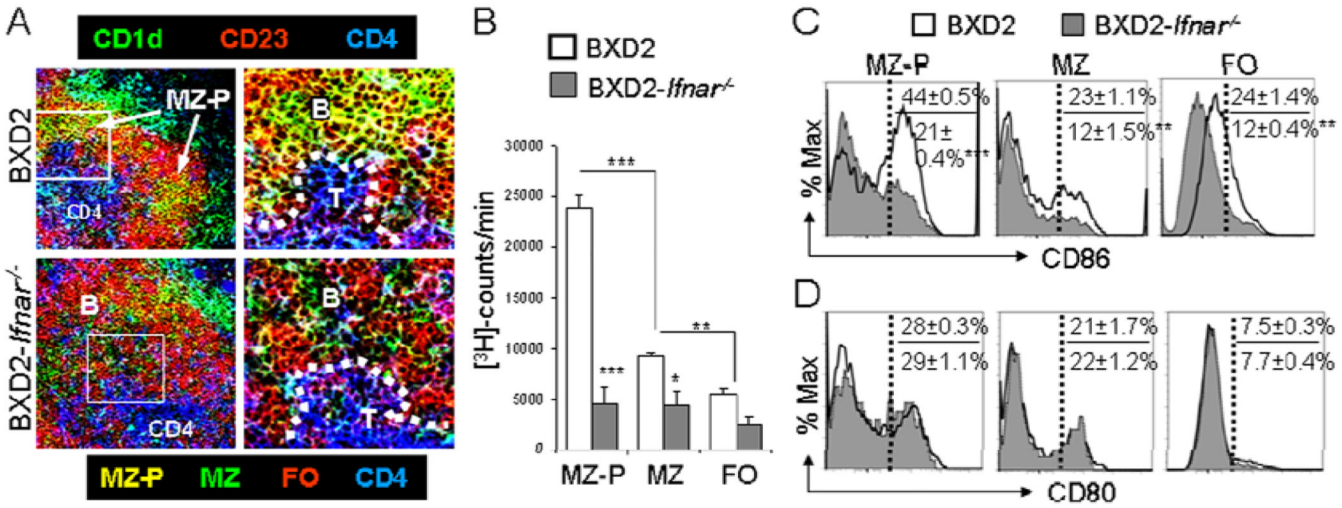

Figure 4.

Potent costimulatory MZ-P B cells at T-B border at the pre-GC stage depends on type I IFN. **A**, Histological analysis of FO ($CD23^{+}CD1d^{-}$, *red*), MZ ($CD23^{-}CD1d^{+}$, *green*), MZ-P (CD23+$CD1d^{+}$, *yellow*) B cells, and CD4 (*blue*) T cells located on a representative spleen tissue section from a representative BXD2 and a BXD2-*Ifnar*$^{-/-}$ mouse. CD4 and B cells are denoted as T and B, respectively. The boxed area in the left panels are magnified to show junction at the T-B border, denoted as white dashed line. **B**, Tritiated thymidine proliferation assay of irradiated MZ-P, MZ, and FO B cells from BXD2 and BXD2-*Ifnar*$^{-/-}$ mice co-cultured with CD4 T cells and an agonistic anti-CD3 antibody for 48 hours (N=3 independent experiments from two mice per experiment, * p<0.05, **p<0.01, *** p<0.001 between BXD2 and and BXD2-*Ifnar*$^{-/-}$ or between the indicated comparison). **C, D**, Representative flow cytometry analyses indicating CD86 (**C**) and CD80 (**D**) expression on splenic MZ-P, MZ, and FO B cells from BXD2 and BXD2-*Ifnar*$^{-/-}$ mice. Results are shown as average ± SEM of $CD86^{+}$ or $CD80^{+}$ B-cell subpopulation from BXD2 (*numerator*) and BXD2-*Ifnar*$^{-/-}$ (*denominator*) mice (**p<0.01, ***p<0.001).

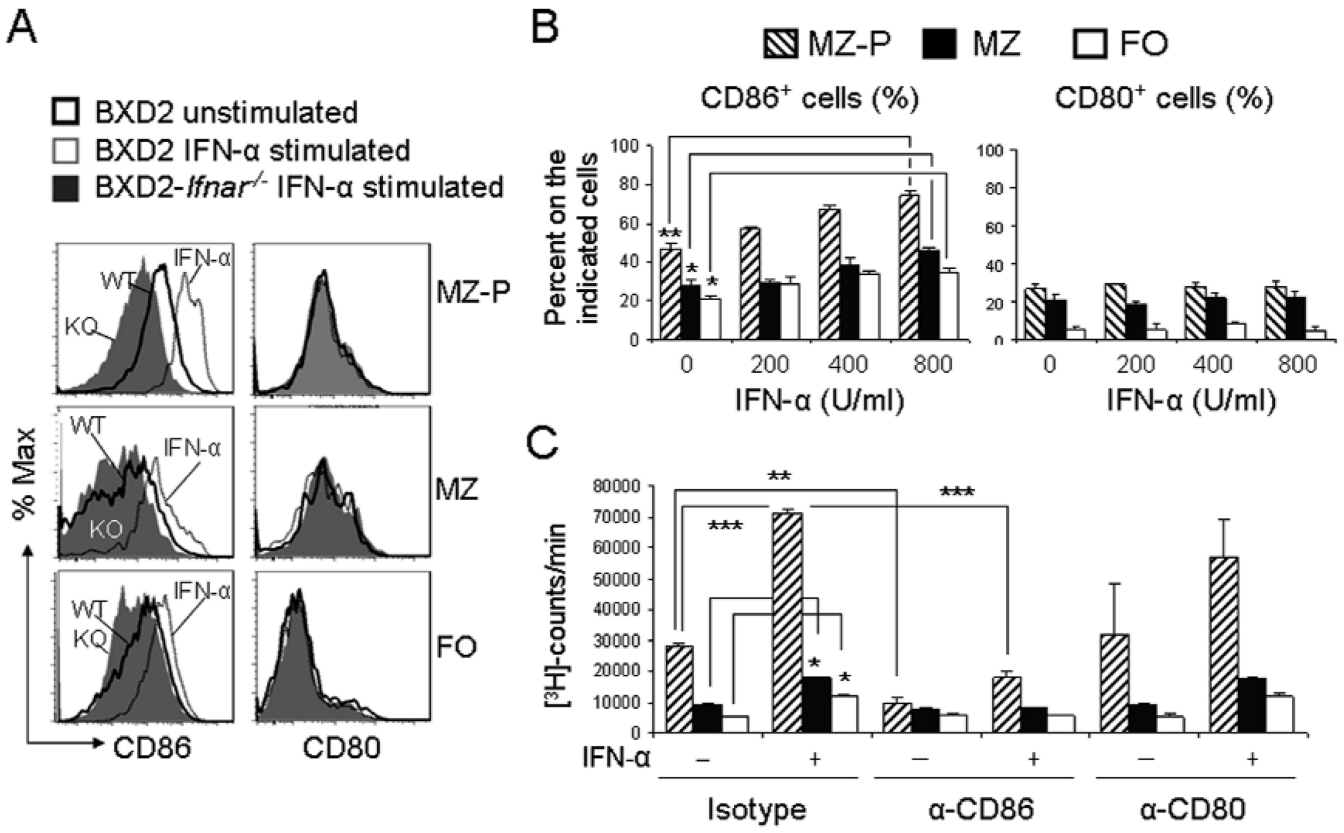

Figure 5.

IFN-α-induced costimulatory function of MZ-P B cells was suppressed by CD86 neutralization. **A**, FACS sorted MZ-P, MZ, and FO B cells from BXD2 and BXD2-*Ifnar*$^{-/-}$ mice were stimulated with medium or IFN-α (400 U/ml), as described in Materials and Methods. Results are shown as the representative FACS histograms showing the cell surface expression of CD86 and CD80 in the indicated population of B cells. **B**, Bar graphs showing the IFN-α-induced dose dependent induction of the expression of CD86 and CD80 on sorted MZ-P, MZ, and FO B cells. **C**, Tritiated thymidine proliferation assay of irradiated MZ-P, MZ, and FO B cells from BXD2 and BXD2-*Ifnar*$^{-/-}$ mice co-cultured with CD4 T cells and an agonistic anti-CD3 antibody for 48 hours. Sorted B cells were stimulated with or without IFN-α first as described in Materials and Methods. Cells were cultured in the presence of rat IgG2a κ isotype control (10 μg/ml), anti-CD86 (10 μg/ml), anti-CD80 (10 μg/ml). All results are shown as mean ± SEM (N=3 independent experiments from two mice per experiment, * $p<0.05$, ** $p<0.01$, *** $p<0.001$ between the indicated comparison).

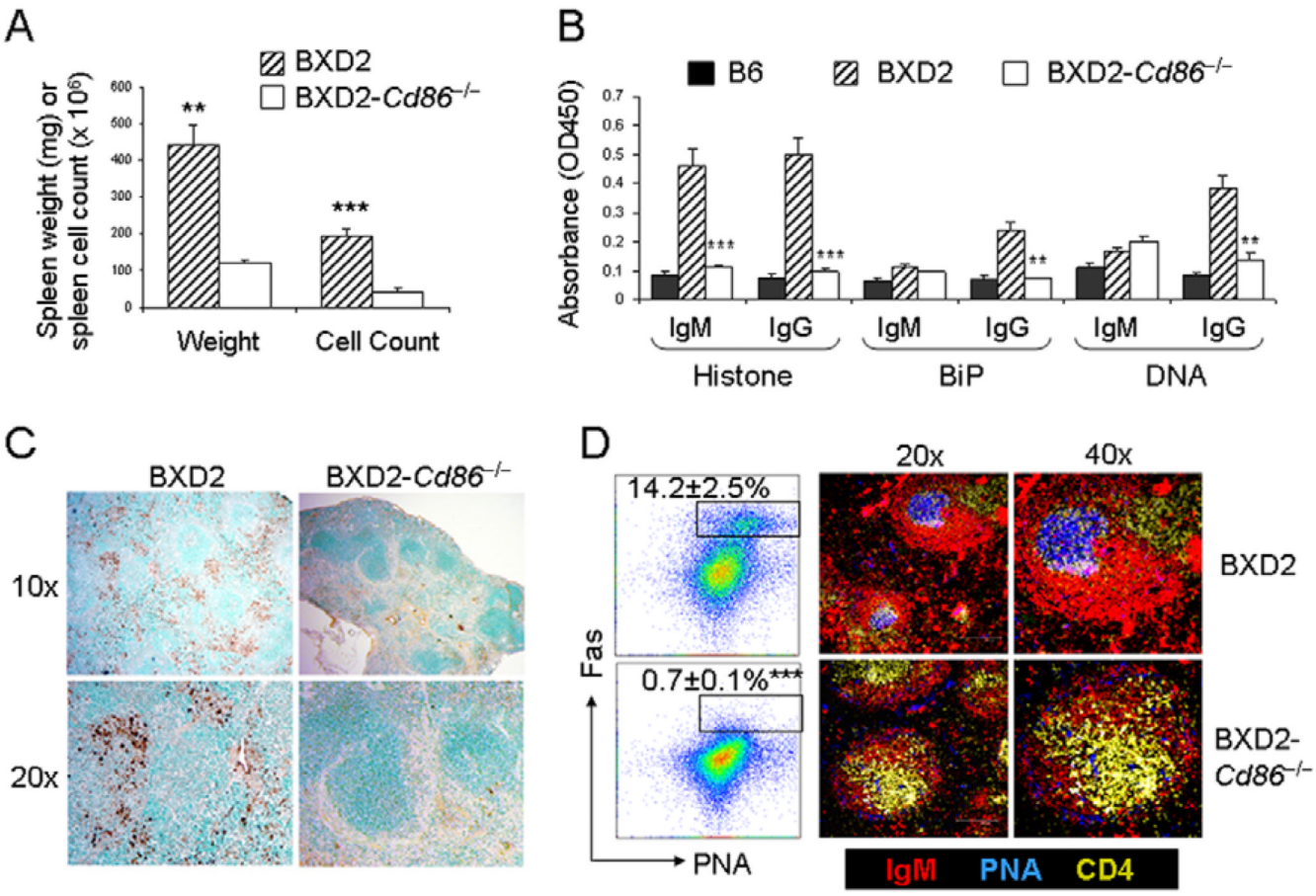

Figure 6.

CD86 is critical for autoantibody and GC formation in BXD2 mice. Spleens from BXD2 and BXD2-*Cd86*$^{-/-}$ mice (10-mo-old) were harvested. **A**, Spleen weight and the total cell count, as determined by a hemocytometer, between BXD2, and BXD2-*Cd86*$^{-/-}$ mice are shown. **B**, Titers (O.D. absorbance units) of serum autoantibodies to histone, BiP, and DNA from B6, BXD2, and BXD2-*Cd86*$^{-/-}$ mice. **C**, Representative (1 of N=6) histological analysis of spleen tissue sections from BXD2 and BXD2-*Cd86*$^{-/-}$ immunohistochemically stained as described in Materials and Methods with anti-IgG antibody at 10× and 20× objective lens magnifications. **D**, Left: Flow cytometry analysis of splenic GC B cells (Fas^+PNA^+, gated on $CD19^+$ B cells first) from BXD2 and BXD2-*Cd86*$^{-/-}$ mice with indicated percentages of Fas^+PNA^+ cells. Right: The corresponding representative (1 of N=6) histological analysis of spleen sections from BXD2 and BXD2-*Cd86*$^{-/-}$ mice at 20× and 40× objective lens magnifications. All results are shown as mean ± SEM (** $p<0.01$, ***$p<0.001$ between BXD2 vs BXD2-*Cd86*$^{-/-}$, N=6).